International Journal of Nanoelectronics and Materials
Volume 16, No. 3, July 2023 [725-736]

Synthesis of Zinc Sulfide Luminescent Nanoparticles Using Zinc Metal Complexes of S-benzyl Dithiocarbonate via Microwave Irradiation Route

Ranjana Sharma Goswami[2], Y. C. Goswami[1*] and D. Kumar[1]

[1]PG Department of Chemistry, SMS Govt Science College, Gwalior M P India 474001
[2] School of Sciences, ITM University, Turari, Gwalior, MP 474001, India

Received 16 May 2022, Revised 15 October 2022, Accepted 1 November 2022

ABSTRACT

This paper reported highly luminous zinc sulfide (ZnS) nanoparticles grown by microwave-irradiated single molecular precursors. The precursor was obtained by Schiff bases of S-benzyl dithiocarbazate (SBDTC) ligand using 5-Bromo-4-hydroxy-3-methoxy-2-nitro Benzaldehyde; 4NNbiscyno diethylamino benzaldehyde and p-amino acetophenone. The nanoparticles obtained were characterized by X-ray diffraction studies for structural analysis, transmission electron micrographs (TEM) for morphological analysis, and UV-Vis spectra for optical analysis. X-ray diffractograms exhibit mixed structures analysis (wurtzite and cubic) for particles obtained using 5-Bromo-4-hydroxy-3-methoxy-2-nitro benzaldehyde and 4NNbiscyno diethylamino benzaldehyde. However, the particles obtained by p-amino acetophenone Schiff bases of SBDTC exhibit only wurtzite structure. Variation in optical properties is also observed with the precursors used. The excellent optical properties of ZnS nanoparticles signify the role of microwave irradiation in synthesis. The Photoluminescence (PL) study shows the luminescence in the visible region and the maximum intensity for ZnS particles obtained by zinc complex of p-amino acetophenone Schiff base of S-benzyl dithiocarbazate. The microwave-assisted process can be used for large-scale production of nanoparticles for emitting light in the visible region in various detecting and sensing applications

Keywords: Chalcogenides**;** Schiff bases; Single-molecule precursor; Zinc Sulfide; nanoparticles.

1. INTRODUCTION

Zinc Sulfide (ZnS) is an environmentally friendly material, chemically more stable, and on the technological front, excellent semiconductor nanomaterials with a broad direct band gap (E_g=3.68eV) [1-3]. High refractive index., excellent transmittance in the visible range [4], and good exciton binding energy (40meV) [5, 6] make Zinc sulfide nanoparticles fit for a variety of optoelectronic uses. It is one of the oldest and probably one of the most important materials in the electronics industry, with many applications in phosphors electronics devices. At ambient conditions, ZnS exhibit two different crystal structures, a cubic phase and wurtzite. Compared with the cubic phase, wurtzite ZnS has much better optical properties; however, it is less stable than the cubic structure. At ambient conditions, wurtzite of smaller size can quickly transform into a cubic structure [7]. Due to their unique properties, ZnS nanocrystals have versatile potential applications [8, 9] in ultraviolet light-emitting diodes[10], solar cells [11,12], field emitters [13], injection lasers [14,15], sensors [16], thin film based electronics devices, electroluminescent devices, and IR windows [17-19]. Many synthesis routes have been

* Corresponding author: ycgoswami@gmail.com

developed for the synthesis of ZnS nanostructures. However, many of them contain toxic chemicals and harmful by-products [20-24]. Production of large-scale ZnS nanoparticles for various applications is also a challenge. In this paper, we have reported a rapid and large-scale synthesis of optically important ZnS nanostructures obtained through microwave decomposition of single molecular precursors obtained using zinc complexes of 5-Bromo-4-hydroxy-3-methoxy-2-nitro Benzaldehyde,4NNbiscyno diethylamino benzaldehyde p-amino acetophenone Schiff base of S-benzyl dithiocarbazate.

2. MATERIAL AND METHODS

2.1 Materials used

All the chemicals used were of analytical grade. Potassium hydroxide, Carbon disulfide, Ethanol, Dimethyl Sulfoxide (DMSO), Zinc acetate, Hydrazine hydrate, Para Aminoacetophenone, 5-Bromo-4-hydroxy-3-methoxy-2-nitro Benzaldehyde, 4-NN biscynodiethylamino benzaldehyde were obtained from CDH fine chemical /Ranbaxy India and used as such without further purification.

2.2 Instruments used

Microwave, Ultrasonicator, Bath with magnetic stirrer

2.3 Experimental

Synthesis of Cadmium sulfide (CdS) nanoparticles single molecular complex and obtaining CdS nanoparticles consist of several steps. Firstly, the S-Benzyl dithiocarbazate (SBDTC) ligand was synthesized. The group has already reported the synthesis of ligands obtained by S-Benzyl dithiocarbazate and their Schiff bases [25-27]. This SBDTC ligand was used to obtain Schiff bases of 5-Bromo-4-hydroxy-3-methoxy-2-nitro Benzaldehyde (Schiff base 1); 4NNbiscyno diethylamino benzaldehyde (Schiff base 2), *and* p-amino acetophenone (Schiff base 3). In the third step, these Schiff bases were used to make complexes with Zinc salt. Zinc complex 1 was obtained using Schiff base 1 of 5-Bromo-4-hydroxy-3-methoxy-2-nitro Benzaldehyde; Zinc Complex 2 was obtained using Schiff base 2 of 4NNbiscyno diethylamino benzaldehyde and Zinc Complex 3 was obtained using Schiff base of p-amino acetophenone precursors. These Complexes were used to synthesise ZnS nanoparticles by irradiated microwave decomposition.

The potassium salt of dithiocarbazic acid was used to obtain a ligand-based on S-benzyl dithiocarbazate. Ethanol and distilled water were mixed in a ratio of 9:1. Finally, the potassium salt of dithiocarbazic acid was added to about 140 ml solution and stirred thoroughly using a magnetic stirrer.

This mixture was then kept at a low temperature with the help of ice water. 22.8g of Potassium hydroxide and 20g of Hydrazine hydrate were added slowly to the cooled mixture. The solution was stirred well for a few hours. Now the Carbon disulfide (CS2) solution was prepared by adding 30.4g CS_2 in 25 ml ethanol. The CS_2 solution was added dropwise into a cooled hydrazine hydrate and KOH solution using a dropping funnel. The mixture was kept idle after continuous stirring for another one h. The oily layer, yellow in colour, was separated using a separating funnel and kept in the ice bath to initiate the reaction, 25 ml of Benzyl chloride was added to the mixture and stirred for 10 minutes until a white product formed and separated. The resultant mixture was washed multiple times with water to obtain the final product and then filtered. Finally, the product was dried by exposing it to air.

Synthesis of Schiff base of SBDTC ligand

To prepare the S-benzyl dithiocarbazate solution, a concentration of 0.02M (3.96g) of S-benzyl dithiocarbazate was dissolved in 120ml of ethanol at a temperature of 40°C. The mixture was thoroughly mixed to obtain the solution. This solution was then divided equally into three parts.

Three solutions of Schiff base 1, Schiff base 2, and Schiff base three were prepared by dissolving each Schiff base in ethanol at a concentration of 0.2M, using separate flasks.

Next, one part of the S-benzyl dithiocarbazate solution was added to each Schiff base solution (Schiff base 1, Schiff base 2, and Schiff base 3). The resulting mixtures were stirred magnetically at 60°C for 5 hours. After the reaction time, the medicines were allowed to cool to room temperature. Once the solutions were sufficiently cooled, they were washed several times with water to remove any impurities. Subsequently, the answers were filtered to obtain the final products.

Synthesis of Zinc ion complexes

For zinc complex preparation, Zinc acetate was used as the starting material. 0.5mM of salt solution was prepared in 25ml of ethanol. Constant stirring was done to get a fine answer. Another explanation of Schiff base is prepared by dissolving 1M Schiff base 1, Schiff base 2, and Schiff base 3 in ethanol (30ml). Both resolutions were added with uninterrupted stirring. After 3 hours, the white precipitate was obtained. The white precipitate was washed thoroughly with ethanol and filtered. Three zinc complexes were obtained, namely Zinc complex of Bromo-4-hydroxy-3-methoxy-2-nitro Benzaldehyde (Zinc Complex 1), 4NNbiscyno diethylamino benzaldehyde (Zinc Complex 2, *and* p-amino acetophenone (Zinc Complex 3).

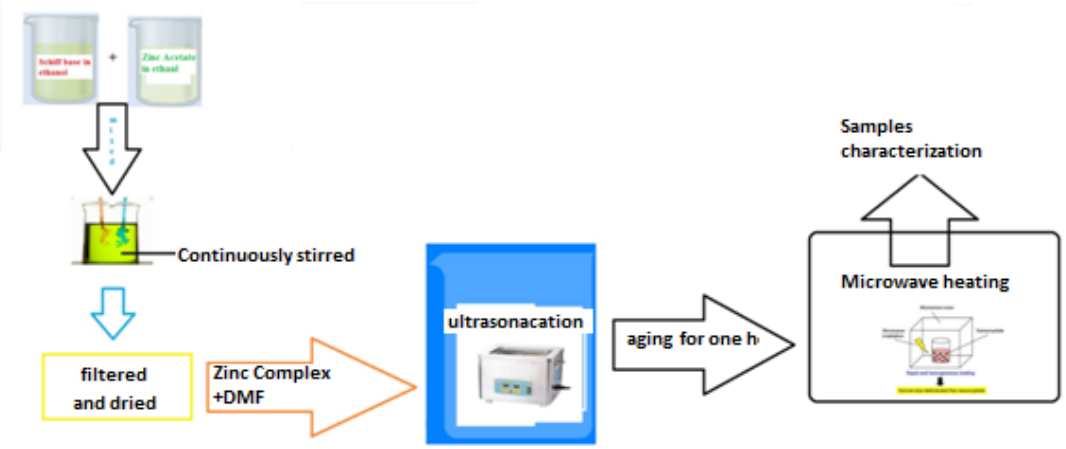

Fig. 1. Block representation of process of synthesis of ZnS nano structures

Microwave heating is used for the decomposition of precursors. In microwave heating, 1g of Zinc Complex was dissolved in 20ml dimethyl sulfoxide in a 100ml beaker. The solution was thoroughly mixed using ultrasonication for 30 minutes at 75°C and then kept idle for another 30 min. Finally, the ultrasonically treated solution was kept in the microwave oven to irradiate with 720W microwaves for 10 min. Methanol and chloroform were used several times for washing. Steps are shown through the block diagram in Fig.1.

The samples were collected and analyzed for structural studies by X-ray diffractograms, morphological studies by TEM, and optical studies by UV-Visible & PL spectroscopy. X-ray diffractograms were obtained using an analytical X-ray diffractometer, X PertPro PAN in the 2θ range 20 ^{0}C to 80 ^{0}C with Cu Kα radiation of wavelength 1.546 Å. Transmission electron

microscopy and high-resolution TEM were used to obtain micrographs using TECHAI G2 F20 operated at 300 kV. Perkin Elmer PL-55 fluorescence spectrophotometer at excitation wavelength 300 nm was used to obtain emission spectra from 200 nm to 800 nm.

3. RESULTS AND DISCUSSION

Microwave heating is used for synthesizing ZnS nanoparticles. Microwave heating plays a vital role in encouraging the breaking of chemical bonds in the complex. Dimethyl sulfoxide (DMSO) solvent has a high boiling point and a permanent dipole moment; hence, it is beneficial as a polar solvent. DMSO is a brilliant absorber of microwave irradiation. This results in direct heat up of the opposite solution [25-29]. The polar solvent DMSO acts as both dispersion media and reaction media. . Adding Dimethyl sulfoxide to the reaction medium results in the axial growth of ZnS. Thus, it is clear from this reaction that adding a catalytic amount of polar solvents could generate heating, which in turn helps in the decomposition of the metal complexes [29-31]. The product yield was calculated at about 40%, and the melting point at about 123°C.

3.1 Structural studies

X-ray diffraction patterns of ZnS nanoparticles, synthesized using Zinc Complex 1, Zinc Complex 2, and Zinc Complex 3, respectively, are shown in Fig 2(a-c). Sharp peaks are observed in Fig 2(a). The (100), (002), (101), (102), (110) (103) and (112) peaks are identified for wurtzite structure. Along with this, cubic peaks are also observed at (200), (220), (311), and (400). This shows mixed-phase formation for ZnS nanoparticles [25, 28-33]. Rapid decomposition of the precursor may cause the mixed phase ZnS structures. Figure 2(c) shows the X-ray diffractogram of ZnS nanoparticles obtained from complex 3. The peaks are broad and have small intensities. Three peaks of wurtzite structure, namely (002), (110), and (103), are observed. Broadness in the peaks indicates the formation of small size particles. Rock salt cubic structure formation is possible under modest external pressure or the pressure generated by the precursor. The precursor has the advantage of generating excess pressure that converts the wurtzite structure into a cubic structure. Wurtzite zinc oxide transforms into the rock salt structure at relatively modest external hydrostatic pressures. The transformation occurred due to the reduction of the lattice dimensions, resulting in interionic Coulomb interaction that favours the ionic behavior more than the covalent nature. The size of particles is calculated using Debye Scherrer equation 1 for (002) peak. The obtained particle size is estimated to be about 5-8 nm.

$$D_p = \frac{0.94\lambda}{\beta_{1/2} Cos\theta} \quad (1)$$

With Complex 1 and Complex 2, mixed wurtzite and cubic structures peaks are obtained; however, with Complex 3, only wurtzite structure peaks are observed. This indicates the strong structural dependence of ZnS particles with the complex used.

.

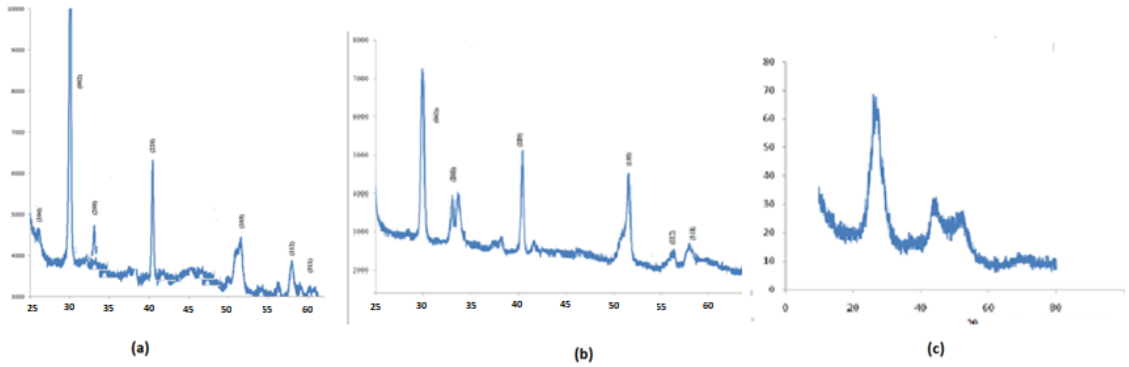

Fig.2 X-ray diffractograms of ZnS nano particles synthesised (using (a) Zinc Complexes 1, (b) Zinc complexes 2 and Zinc Complexes 3).

3.2 Morphological studies using transmission electron microscopy (TEM)

Transmission electron microscopy (TEM) and high-resolution transmission electron microscopy (HRTEM) provide a micrograph for ZnS nanoparticles obtained by metal complex one are shown in Figure 3. Spherical particles are observed with uniform size distribution as shown by histogram. SAED pattern and HRTEM show the crystalline behavior of particles. The

size of the particles is about 25-35nm, as per the TEM micrograph.

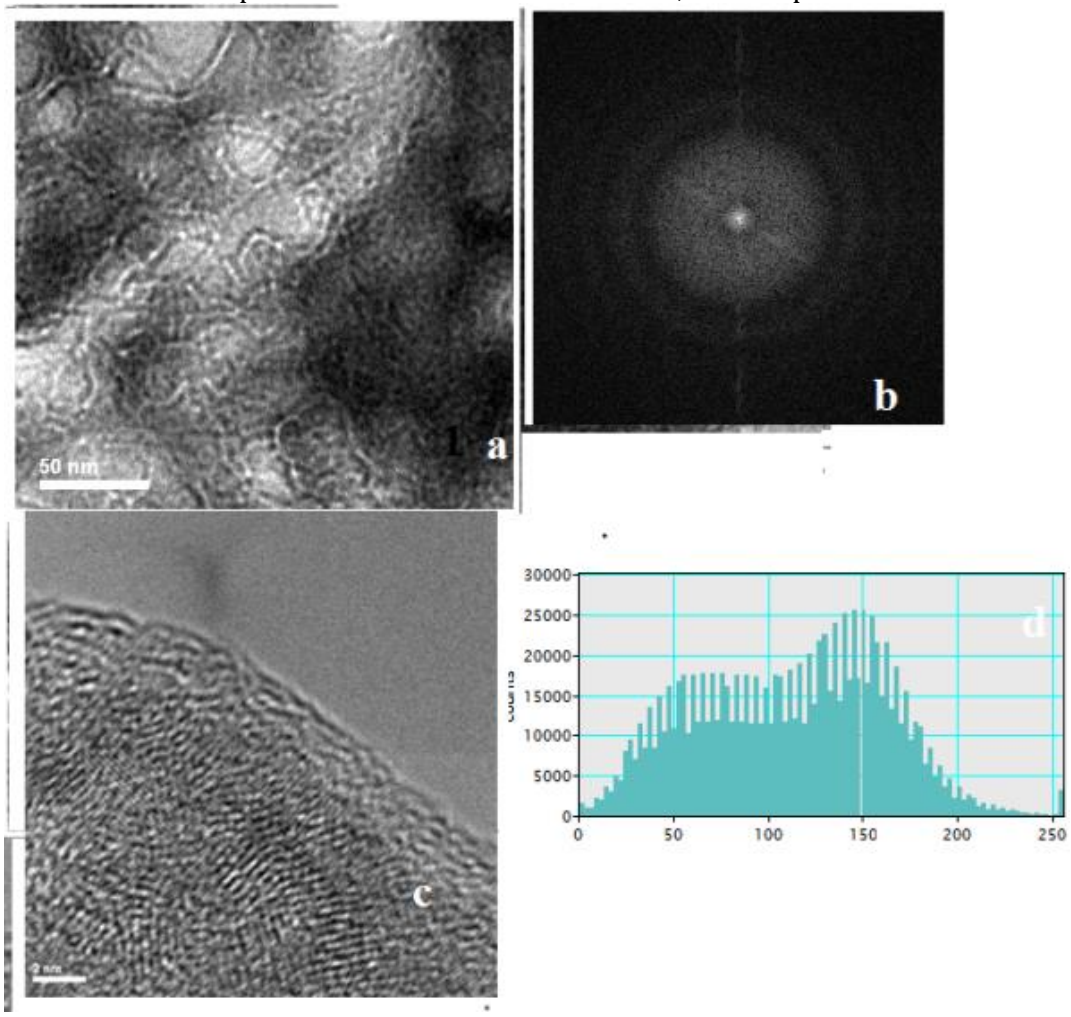

Fig 3 TEM of ZnS particles synthesised using Zinc complex 1 (a) TEM (b) SAED pattern (c) HRTEM micrograph (d) histogram.

HRTEM of ZnS nanostructures obtained using metal complex two along with selected area (electron) diffraction (SAED) and histogram patterns are shown in Fig.4. High-resolution lattice images show the formation of suitable quality particles. Bright points are observed in SAED, indicating good crystallinity of the particles. A histogram indicates uniform size distribution of particles [31]. HRTEM micrographs of the ZnS structures, obtained using metal complex 3 shown in Fig 5 with bright and dark fringes, indicate the presence of crystallinity.

The TEM/HRTEM results indicate the good crystallinity in ZnS nanoparticles obtained with complex 3. π conjugation in acetophenone helps obtain good quality nanoparticles compared to other Benzaldehyde complexes.

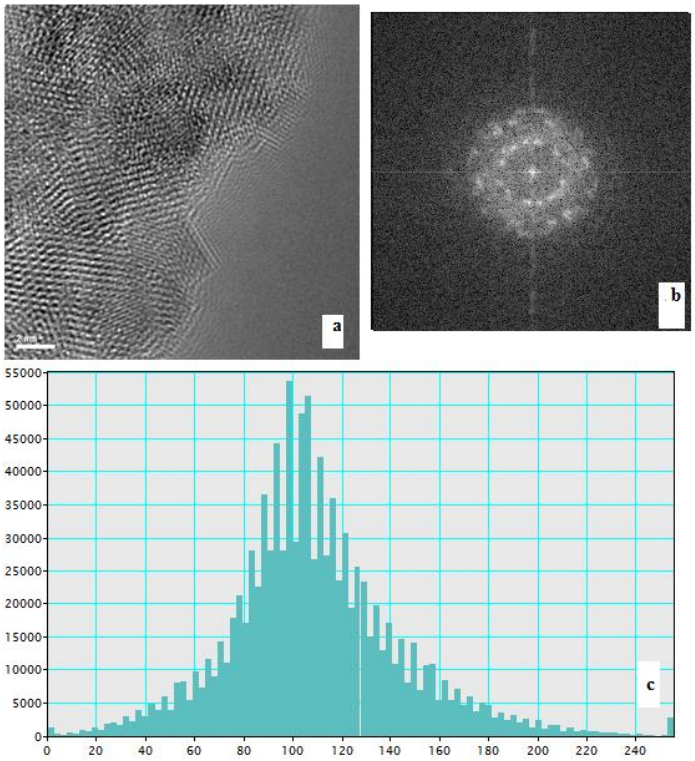

Fig.4. HRTEM image Histogram of ZnS particle obtained using Zinc complex 2.

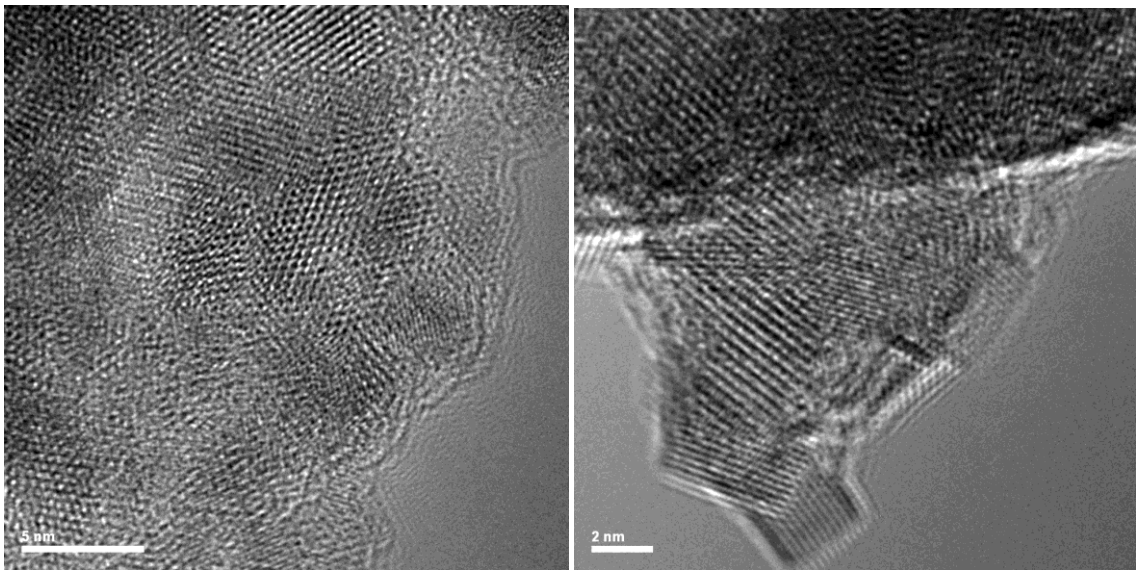

Fig5. TEM and HRTEM of ZnS nanoparticles synthesis using zinc complex 3

3.3 Optical Studies

Optical spectra of ZnS particles synthesised using Zinc complex 1, 2 and 3 are shown in Fig. 6.

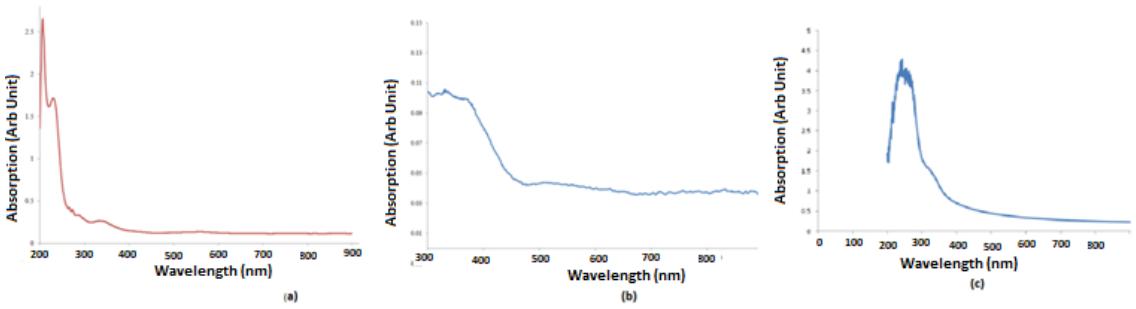

Fig6. Optical absorption spectra of ZnS nanoparticles (a) Zn Complex 1, (b) Zn Complex 2 and (c) Zn Complex 3.

In Fig 6 illustrates the absorption spectra for different ZnS structures obtained using various Zinc complexes. In Fig. 6(a), absorption initiates at 225 nm and exhibits another peak at around 245 nm. Subsequently, sharp absorption occurs at higher wavelengths, and well before the visible region, absorption reduces to a minimum. Notably, the particles are transparent to visible light, as mentioned in references [32-35].

The absorption spectrum for ZnS structures obtained using Zinc complex two is shown in Fig. 6. (b) Absorption is not very sharp. However, the particles are almost transmission in the visible region.

In Fig. 6(c), the absorption spectrum for ZnS structures obtained using Zinc complex three is displayed. Here, sharp absorption occurs at about 300 nm due to the small size of the particles. Nanoparticle size can be estimated using empirical models [47] based on the information provided in the absorption spectra [47]. The particle size using the first excitonic absorption peak in the UV–Vis spectra according to Equation (2) can be calculated

$$D = (9.8127X10^{-7})\,\lambda_{exc}^2 - (1.7147X10^{-3})\lambda_{exc}^2 + 1.0064\lambda_{exc} - 194.84 \quad (2)$$

Where λexc (nm) is the wavelength of the first excitonic absorption peak of the ZnS Quantum dot, D (nm) is the size of a given nanocrystal sample. Data reveal that the size of nanoparticles is about 26.2nm. The results are also confirmed by Heinlein's empirical model [48] using Equation (3).

$$D = \frac{0.1}{(0.1338 - 0.0002345\lambda_{exc}} \quad (3)$$

Where D (nm) is the sample size, and λexc is the wavelength of the first excitonic absorption peak of Zinc sulfide QDs.

3.4 Luminescence studies for Optoelectronic applications

The previous discussions have revealed a significant dependence of ZnS nanoparticle structures and optical properties on the choice of precursor. The designs are almost spherical or hazy, so only a little information can be obtained from TEM; however, a Good High-resolution micrograph and observance of dark and bright fingers favour the crystalline nature. ZNS structures are mixed (wurtzite and cubic) in almost all places. Optical absorptions are sharper for some samples than others, where absorptions are gradual. Results are compiled in Table 1.

Table 1 ZnS nanoparticles grown by different precursors

Precursor used	**Samples**	**Structure**	**Shape**	**Optical Absorption**
[Zn^{II} (Br Hy Me Ni PhMeSbdtcz)$_2$] Complex 1	Zinc Complex 1	Mixed Wurtzite and cubic	Almost Spherical shape	Sharp at about 280 nm
[Zn^{II}(NNBiCDEAmPhMeSbdtcz)$_2$] Complex 2	Zinc complex 2	Mixed Wurtzite and cubic	Almost Spherical shape,nice SARD pattern	At 380 nm
[Zn^{II} (AmPhMeSbdtcz)$_2$] Complex 3	Zinc complex 3	Wurtzite	hazy	Sharp at 390 nm

The photoluminescence studies conducted on ZnS nanostructures obtained using three different zinc complexes, namely [ZnII (Br Hy Me Ni PhMeSbdtcz)2] (Zinc Complex 1), [ZnII(NNBiCDEAmPhMeSbdtcz)2] (Zinc complex 2), and [ZnII (AmPhMeSbdtcz)2] (Zinc complex 3), have yielded interesting results, as depicted in Figure 7.

For Zinc Complex 1 and Zinc Complex 2, the photoluminescence spectra exhibit luminescence peaks at 467nm and 545nm, respectively, indicating emission at these wavelengths. Moreover, these ZnS nanostructures exhibit a shift towards higher wavelengths, making them suitable for optoelectronic applications. Remarkably, the intensity of luminescence is nearly identical for both samples.

On the other hand, ZnS prepared using Zinc Complex 3 shows a significantly higher maximum photoluminescence (PL) intensity, increasing multiple times and observed at around 470nm. However, the peak is broad and relatively small in comparison. This behavior can be attributed to the influence of π conjugation in the complex, which contains a lone pair of electrons causing a bathochromic shift towards longer wavelengths. The presence of excellent π conjugation in complex 3 enhances its luminescence properties.

These findings indicate that the ZnS nanoparticles synthesized from these complexes hold promise for various optoelectronic applications due to their unique luminescence characteristics and tunable emission wavelengths.

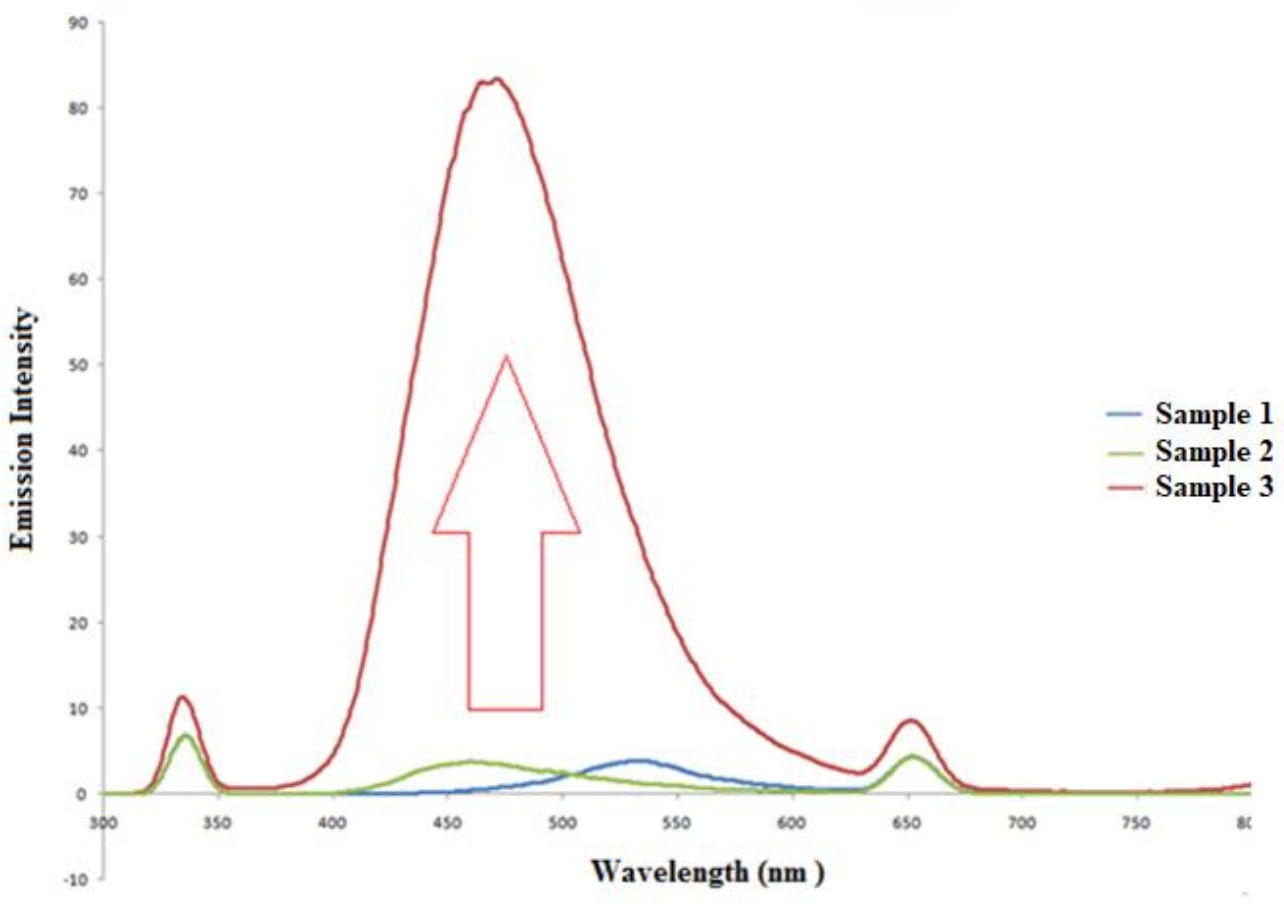

Fig. 7 Luminescence spectra for ZnS samples synthesized using (a) Zn Complex 1 (b) Zn Complex 2 and (c) Zn Complex 3.

Conclusions

ZnS nanostructures were synthesised using microwave irradiation of Dithiocarbazate ligand as single source precursor. It has been reported that luminescence strongly depends on the complex used as a precursor, keeping synthesis conditions almost identical to the shape. Use of DMSO for microwave irradiation helps to decompose precursors very quickly in the nanoparticles. Dominantly spherical nanostructures of excellent crystallinity were observed. Particles showed mixed structures (wurtzite and cubic). Optical properties also vary with the precursors used and are based on good sharp absorption transition. It can be said that good-quality ZnS nanoparticles can be obtained using microwave irradiation for various optoelectronic applications. A PL study was performed for some of the samples. Samples give luminescence in the visible region, and intensity is maximum for ZnS particles obtained using [Zinc complex 3] precursor. The method can be utilised for large-scale production of ZnS nanoparticles at relatively low temperatures. These particles emit light in visible regions in various detecting and sensing applications.

Acknowledgements

The authors acknowledge the PC-ray research centre of ITM University Gwalior, UGC-DAE Consortium for Scientific Research and School of Material Science, and the University of Manchester UK for providing characterisation facilities. The authors also thank MPCST, Bhopal, MP, India, for funding the research (F.No. A/RD/RP-2/305).

REFERENCES

1. Peng, W.Q., Cong, G.W., Qu, S.C., Wang, Z.G., Opt. Mater. vol **29**,(2006)pp. 313-317.
2. Bhargava, R.N., Gallagher, D., Phys. Rev. Lett. Vol. **72** (1994) pp. 416-419.
3. Geng, B.Y., Zhang, L.D., Wang, G.Z., Xie, T.; Zhang, Y.G., Meng, G.W., Appl. Phys. Lett. vol **84**, (2004) pp. 2157-2159.
4. Bisauriya R., Verma D., Goswami Y. C., J Mater Sci: Mater Electron. Vol **29**, (2018) pp.1868–1876.
5. Kumar N., Purohit, L.P., Goswami, Y.C., AIP Conference Proceedings. Vol **1675**, (2015) pp. 020030.
6. Zhu, H., Su, S.C., Yu, S.F.; Zhang, W.F, Ling, F.C.C., IEEE Journal of Selected Topics in Quantum Electronics. Vol **19**, Issue 4 (2013).
7. Reddy, D.A., Kim, D.H., Rhee, S.J., Lee, B.W., Liu, C., Nanoscale Res. Lett. vol **9** Issue 1, (2014) pp.20-26.
8. Kumar, N., Purohit, L.P., Goswami, Y.C., Chalcogenide Letters vol. **12** Issue 6, (2015) pp. 333-338.
9. Kumar, N., Pathak, T.K., Purohit L.P., Swart, H.C., Goswami, Y.C., Nano-Structures & Nano-Objects vol. **16** (2018) pp.1-8.
10. Lo, H.C., Das, D., Hwang J.S., Chen K.H., Hsu C.H., Chen C.F., Appl Phys Lett, vol **83** (2003), pp. 1420–2.
11. Kumar, V., Rajaram, P., Goswami, Y.C. Journal of Materials Science: Materials in Electronics, vol **28** issue 12, pp. 9024-9031
12. Shen, G.Z., Chen, P.C., Bando, Y., Golberg, D., Zhou, C. Chem Mater vol **20** (2008) pp. 6779–83.
13. Goswami, Y.C., Mohapatra, R., Kaundal, J.B. Chalcogenide letters vol **18,** issue 5 (2021); pp. 255-262
14. Chadi D.J. J. Appl Phys vol 38 (1999),pp.2617–8.
15. Sharma, R., Singh, R., Goswami, Y.C., Kumar V., Kumar, D., Journal of the Australian Ceramic Society Vol **57**, 2021, 57 (3), 697-703.
16. Chadi, D.J., Phys Rev. B. vol 59 (1999), pp. 15181–3.
17. Look, D.C., Claflin, B., Alivov, Y.L., Park, S.J. Phys Status Solid (A) vol **201**, (2004) pp.2203–12.
18. Iida S., Yatabe T., Kinto H., J Appl Phys, vol **28**, (1989), pp.L535–7.
19. Georgobiani, A.N., Kotljarevsky, M.B., Kidalov, V.V., Rogozin, I.V., Aminov, U.A., J. Cryst Growth vol **214/215** (2000) pp.516–9.
20. Mitsubishi, I., Shibatani J., Kao, M.H., Yamamoto, M., Yoshino, J., Kukimoto, H., J Appl Phys, vol **29**, (1990)pp. 733–5.
21. Butkhuzi T.V., Tchelidze T.G., Chikoidze E.G., Kekelidze N.P., Phys Status Sol (B), vol **229**, (2002), pp.365–70.
22. Kohikia S., Suzuka T., Kohikia S., Suzuka T., Yamamoto T., Kishimoto S., J Appl Phys, vol **91** (2002), pp.760–3.
23. Kishimoto S., Kato A., Naito A., Sakamoto Y., Iida S., Phys Status Sol (B) vol **229**, (2002), pp. 391–3.
24. Muthukumaran, S., Kumar M. A., Mater. Lett., vol **93**, (2013) pp.223–225 .
25. Sarkar R., Tiwary C.S., Kumbhakar P., Mitra A.K., Phys. Vol **B404** Issue 21, (2009) pp. 3855–3858
26. Yang H, Huang Xiaohui Su X, aTang A., Journal of Alloys and Compounds, vol **402**,(2005), pp. 274–277.
27. Purohit, L. P., Goswami Y. C., Physica E: Low-dimensional Systems and Nanostructures, vol **83**, (2017) pp. 333-338.
28. Sharma R., Singh B., Kumar V., GoswamiY. C., Singh, R., Kumar D.. Advances in Optical Science and Engineering vol **166**, (2014) pp. 575-580.

29. Arora K, D. Kumar D., *J. Saudi Chem. Soc*., vol **15** (2011) 161.
30. Kumar, D., Agrawal, M.C. Singh, R., *Asian J. Chem*., vol **19** (2007) pp.3703.
31. Marx, N.R., Pandian, K., Sivakumar, K., Applied Surface Science vol **257**, issue 7, (2011) pp.2745-2751
32. , *Chem. Mater.* Vol **12** Issue 2 (2000), pp. 564–567,
33. Feldmann, C. Metzmacher, C., *J. Mater. Chem.*, vol **11** (2001),pp. 2603-2606.
34. Sayre, S.L. Raghuwanshi, P.B., Imperial Journal of Interdisciplinary Research (IJIR) vol **2** Issue 3 (2016) pp. 1131-1138.
35. *Xinjuan, L., Likun, P., Sun C. Q.,* Microwave Engineering of Nanomaterials: From Meso scale to Nanoscale, edited Erwann Guenin, CRE Press, pp. 314-378.
36. Yeh, CY, Lu, Z.W., Froyen, S., Zunger, A. Phys Rev B, vol **46**, (1992), 46 pp10086–97.
37. Chen, H., Shi, D., Qi, J., Jia J., Wang B., Phys Lett A vol **373** pp.371–5.
38. Tran, T.K., Park, W., Tong, W., Kyi, M.M., Wagner, B.K., J Appl Phys, vol **81**, (1997), pp. 2803–9.
39. Karazhanov, S.Z., Ravindran, P., Kjekshus, A., Fjellvag, H., Svensson, B.G., Phys Rev B vol **75**, (2007) pp. 155104.
40. Yu, W. W., Qu, L., Guo, W., Peng, X. Chemistry of Materials, vol **15** issue 14 (2003), pp. 854–2860.